Electronic Supplementary Material (ESI) for Physical Chemistry Chemical Physics.

Supplementary Information for: "Design of fast ion conducting cathode materials for grid-scale sodium ion batteries"

Lee Loong Wong, Haomin Chen, Stefan Adams

Department of Materials Science and Engineering, National University of Singapore, Singapore 117575.

*Corresponding author's e-mail: mseasn@nus.edu.sg

1. Rate performance of selected cathode materials with low-dimensional pathways for Na^+ migration

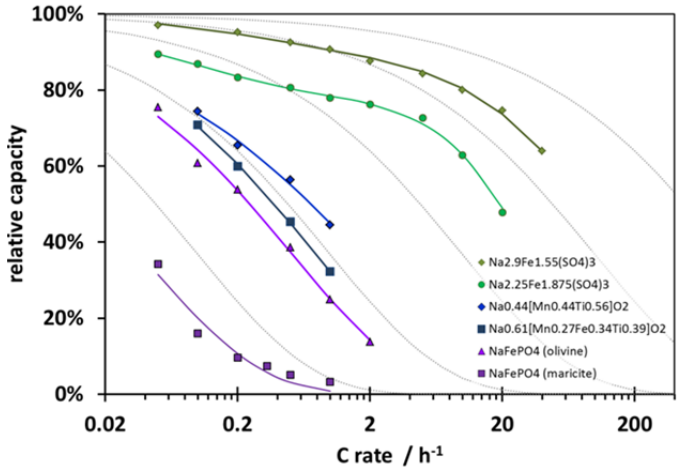

Fig. S1: Comparison of rate performances of various cathode materials with low-dimensional pathways for Na^+ migration: olivine-type $NaFePO_4$ (magenta), two $Na_{0.44}MnO_2$-related cathode materials (blue) and two alluaudite-type cathode materials. Symbols refer to experimental data, solid lines refer to fits to the data based on equation (5a) (or (8a) for the alluaudites). Dotted lines are the same as in Fig. 2.

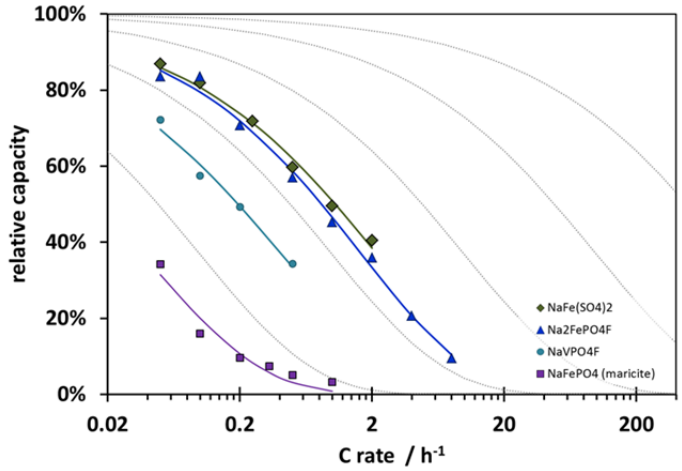

Fig. S2: Comparison of rate performances of various cathode materials with two-dimensional pathways for Na^+ migration: maricite-type $NaFePO_4$ (violet), two tavorite-type cathode materials (blue) and eldfellite-type $NaFe(SO_4)_2$. Symbols refer to experimental data, solid lines refer to fits to the data based on equation (5a). Dotted lines are the same as in Fig. 2.

2. Na^+ pathways in tavorite-type Na_2FePO_4F

Various tavorite-type sodium cathode materials have been reported so far, but since no complete structural characterisation seems to be available for the first reported representative, tavorite-type $NaVPO_4F$,[S1] and the structures for the analogues with other alkali cations $LiVPO_4F$ (SG: *P*-1), Li_2VPO_4F (SG: *C*12/*c*1), $KVPO_4F$ (SG: *Pna*2_1)[S2] and $K_xLi_yVPO_4F$ (SG: *Pnan*) differ significantly, we have chosen to study the Fe-analogue sodium compound, Na_2FePO_4F in space group *Pbcn* based on structure data from ref. S3. As illustrated in Fig. S3, this compound is structurally layered with each layer consisting of face-sharing pairs of Fe-centred octahedra ($Fe_2O_6F_3$), which are connected to each other via corner-sharing with adjacent pairs and PO_4 groups. Consistent with a previous computational study[S4], our model predicts two-dimensional sodium ion pathways in the *ac* plane (*cf*. Fig. S3(a)). Both sodium sites (Na1, Na2) are fully occupied in the as-synthesized compound albeit the presence of a shallow interstitial site between Na1 and Na2 at (0.150, 0.222, 0.967). These Na1-*i*-Na2 sites form local clusters with *ca*. 0.4 eV barriers (*cf*. Fig. 10b) which are then connected to other symmetrically equivalent clusters with a higher barrier of 0.58 eV either via Na1-Na1 or Na1-*i* connections. In the monoclinic pseudo-orthorhombic Na_2MnPO_4F, the (qualitatively similar) pathway transits from 1D (requiring 0.61 eV) to 2D (requiring 0.71 eV).

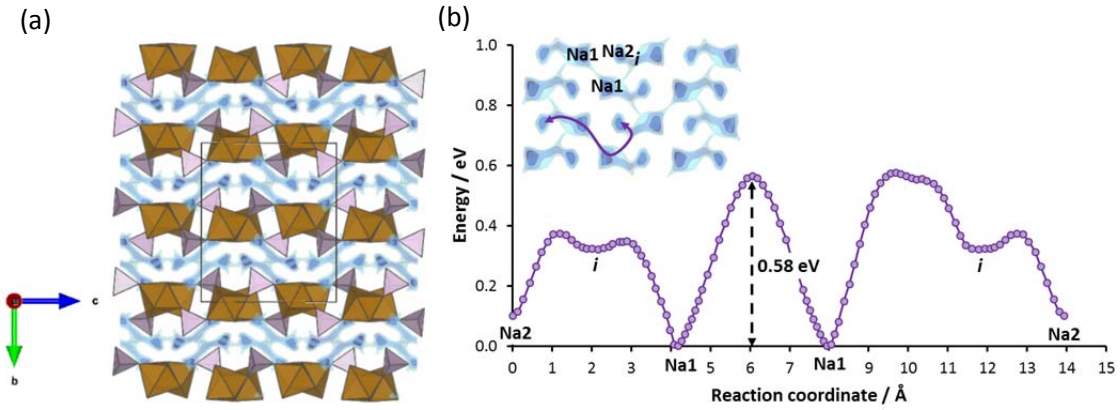

Fig. S3: (a) Layered structure of Na_2FePO_4F (brown octahedra: FeO_6, purple tetrahedra: PO_4) and the corresponding 2D Na^+ pathway in the *ac*-plane represented by blue energy isosurfaces (b) Migration barrier profiles in the 2D pathway. Activation energy for long-range Na^+ transport is 0.58 eV.

[S1] J. Barker, M. Y. Saidi and J. L. Swoyer, *Electrochem. Solid-State Lett.*, 2003, **6**, A1-A4.

[S2] S. S. Fedotov, N. R. Khasanova, A. Sh. Samarin, O. A. Drozhzhin, D. Batuk, O. M. Karakulina, J. Hadermann, A. M. Abakumov and E. V. Antipov, *Chem. Mater.*, 2016, **28**, 411–415.

[S3] B. L. Ellis, W. R. M. Makahnouk, W. N. Rowan-Weetaluktuk, D. H. Ryan and L. F. Nazar, *Chem. Mater.*, 2010, **22**, 1059-1070.

[S4] R. Tripathi, S. M. Wood, M. S. Islam and L. F. Nazar, *Energy Environ. Sci.*, 2013, **6**, 2257-2264.

3. Pathways in $NaVP_2O_7$

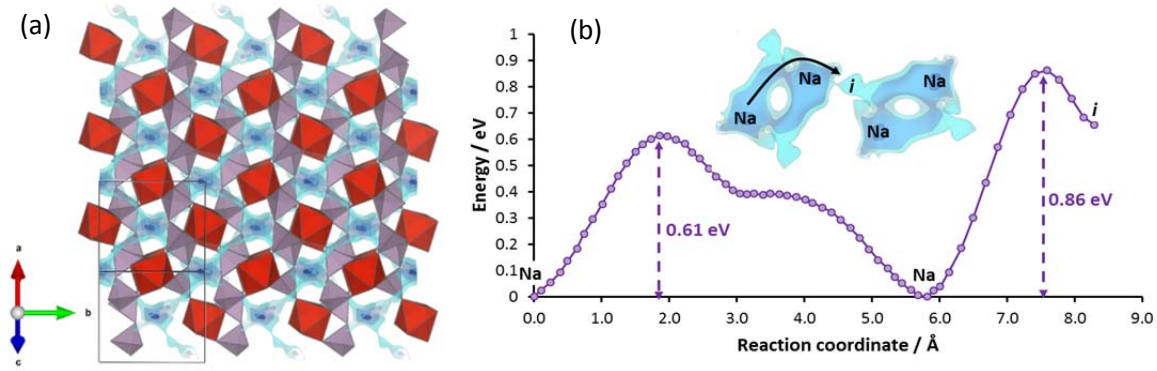

Fig. S4: (a) Crystal structure of $NaVP_2O_7$ (SG: $P2_1/c$) showing corner-sharing PO_4 (purple tetrahedra) and VO_6 (red octahedra) groups (b) Migration pathway of Na^+ within the compound, where an activation energy of at least 0.86 eV is required for long-range transport.

In another study on $NaVP_2O_7$,[S5] a moderate barrier of 0.47 eV was suggested for a migration path connecting two adjacent Na^+ separated by 3.4 Å, although the shortest Na^+-Na^+ distance we have observed in two structures from the same study and ICSD 65696 is significantly higher at 4.1 Å. Based on our BVSE analysis, any long-range Na^+ transport involves migrating through interconnected rings of Na^+-Na^+ pairs (*cf.* inset of Fig. S4) which form a 3D pathway. We assume the barrier mentioned earlier corresponds only to the local intra-ring hop, which from our study should require an activation energy of 0.61 eV. However, our model reveals that for long-range Na^+ conduction, it is necessary to overcome another higher inter-ring barrier of 0.86 eV involving an interstitial site ***i***. Each local ring is connected to four other adjacent rings via four ***i*** sites. Even within each local cluster, Na1-Na1 migration barrier is high at 0.61 eV and involves long hopping distance (> 5 Å). Despite the favourable 3D network, the combination of such unfavourable kinetics for Na^+ transport leads to sluggish bulk diffusion and is therefore the primary reason why this compound falls into the very low rate performance category.

[S5] Y. Kee, N. Dimov, A. Staikov, P. Barpanda, Y.-C. Lu, K. Minami, S. Okada, *RSC Adv.,* 2015, **5**, 64991.

4. Pathways in $Na_2FeP_2O_7$ and $Na_2MnP_2O_7$

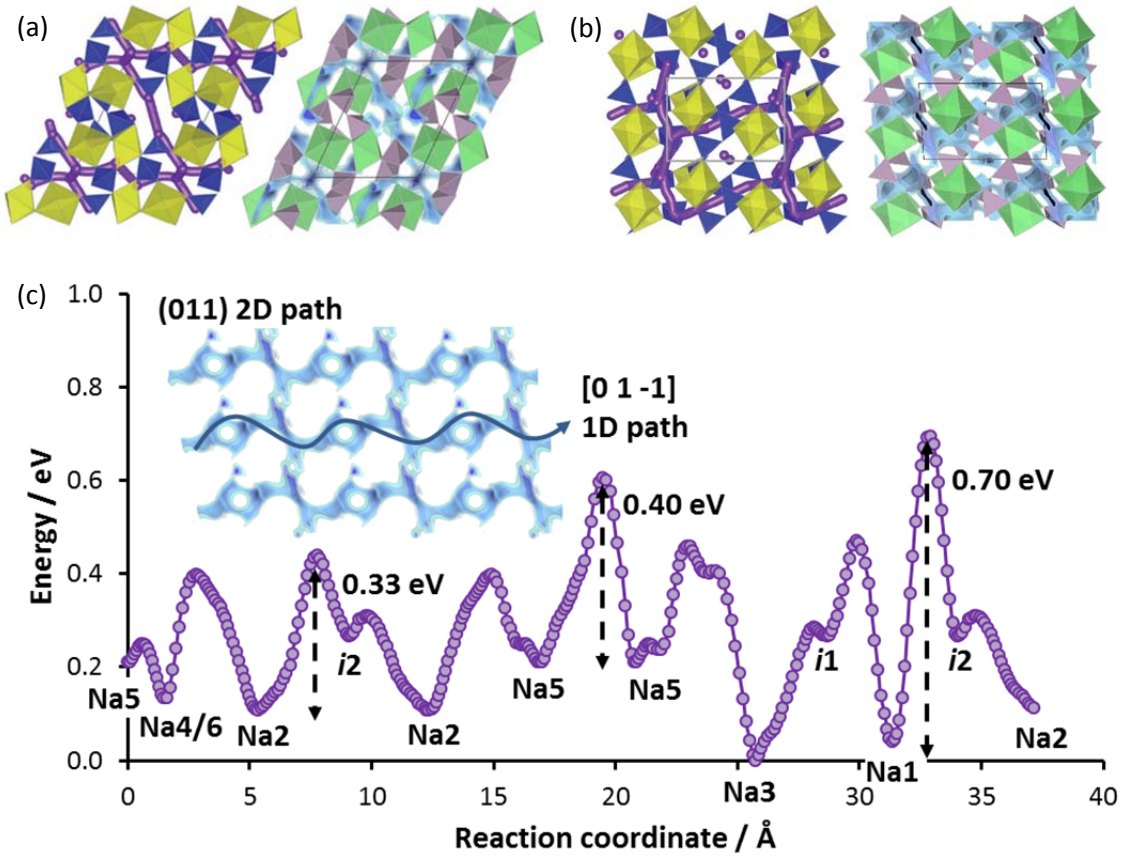

Fig. S5: Projection along (a) *a* axis and (b) *b* axis of $Na_2FeP_2O_7$ comparing pathway topologies studied based on atomistic simulations (left)[S6] and our work (right). (c) The corresponding reaction pathway shows fast 1D Na^+ diffusion along [0 1 -1] channels which are connected via Na5-Na5 path to form 2D (0 1 1) diffusion plane (inset).

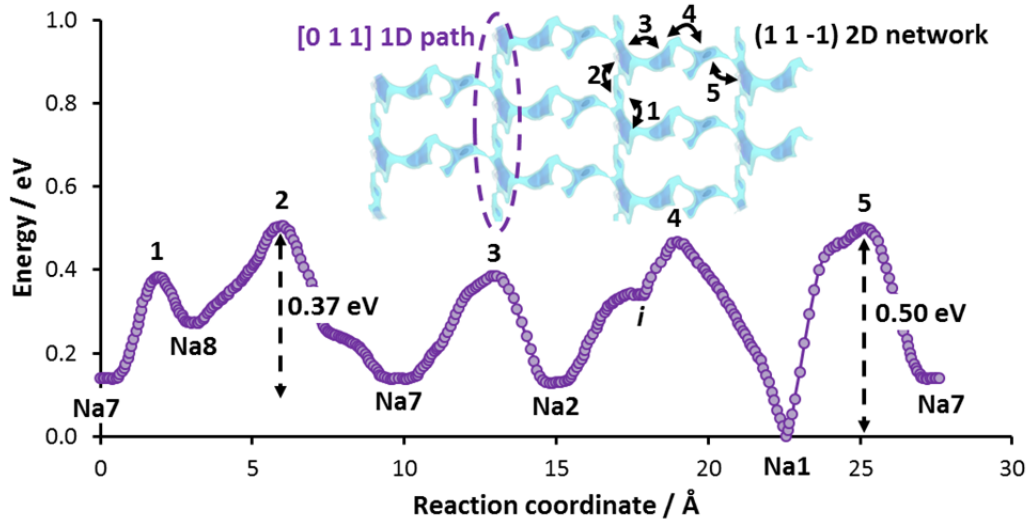

Fig. S6: Like the Fe-analogue, reaction pathway of $Na_2MnP_2O_7$ shows also 1D and 2D percolation (inset), albeit impeded by higher barrier energies.

As discussed in section 3.3.3. of the main paper and shown in Fig. S5, long-range Na^+ transport in this $Na_2FeP_2O_7$ is effectively 2D in the (011) plane, with a particularly low energy ribbon-like 1D path along the [0, 1, -1] direction containing fully occupied Na2 and interstitial site i1.

The limited electrochemical activity of the Mn-analogue $Na_2MnP_2O_7$ (SG: *P*1) is partially due to the overall higher migration barriers involved in the 2D network (Fig. S6). For $Na_2MnP_2O_7$, the minimum energy barrier to be overcome for any long-range Na^+ transport is 0.37 eV (1D) and 0.50 eV (2D), as opposed to the lower barrier of 0.33 eV (1D) and 0.40 eV (2D) in $Na_2FeP_2O_7$.

For $Na_2VOP_2O_7$, we found the underlying pathways to be primarily 1D ribbon-type with high activation energy of 0.74 eV. Most importantly, many of the sodium sites in $Na_2FeP_2O_7$ (Na4/6, Na5) are disordered, in contrast with the Mn and VO analogues where all sodium sites are fully occupied. Such disordered sites are in fact valuable in creating sodium site vacancies facilitating ionic transport.

[S6] J. M. Clark, P. Barpanda, A. Yamada and M. Islam, *J. Mater. Chem. A*, 2014, **2**, 11807-11812.

5. Pathways in $Na_4Fe_3(PO_4)_2P_2O_7$

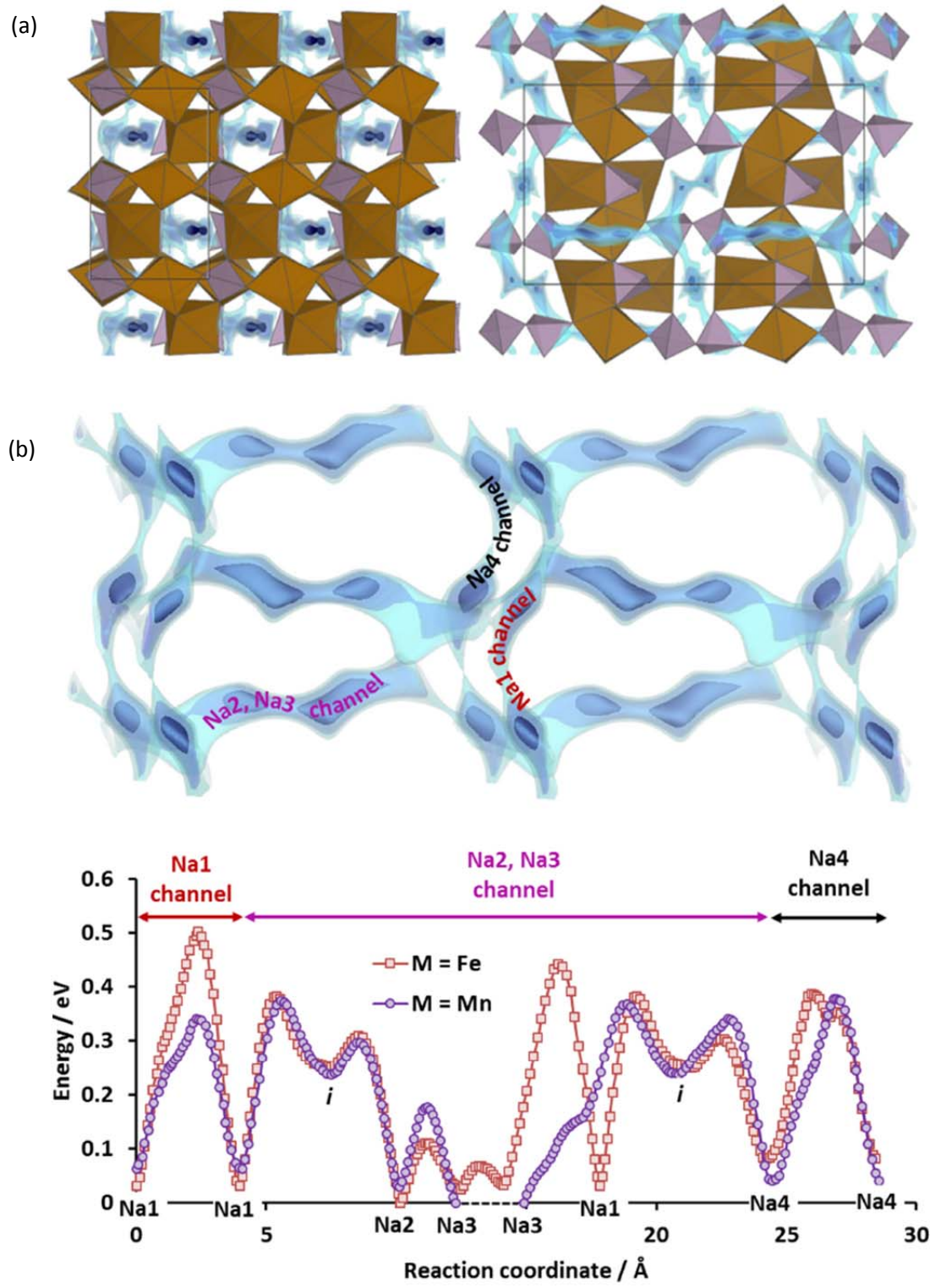

Fig. S7 (a) Na^+ pathways (blue energy isosurfaces) superimposed on a projection of the crystal structure (space group $Pn2_1a$) of $Na_4Fe_3(PO_4)_2P_2O_7$ along (left) *a*- and (right) *b*-direction with black lines marking the unit cell; (b) Each distinct 1D channel in the pathway is labelled with the Na sites involved (top) and the corresponding migration barriers in each channel are shown in the reaction pathway (bottom).

6. Pathways in $Na_4NiP_2O_7F_2$

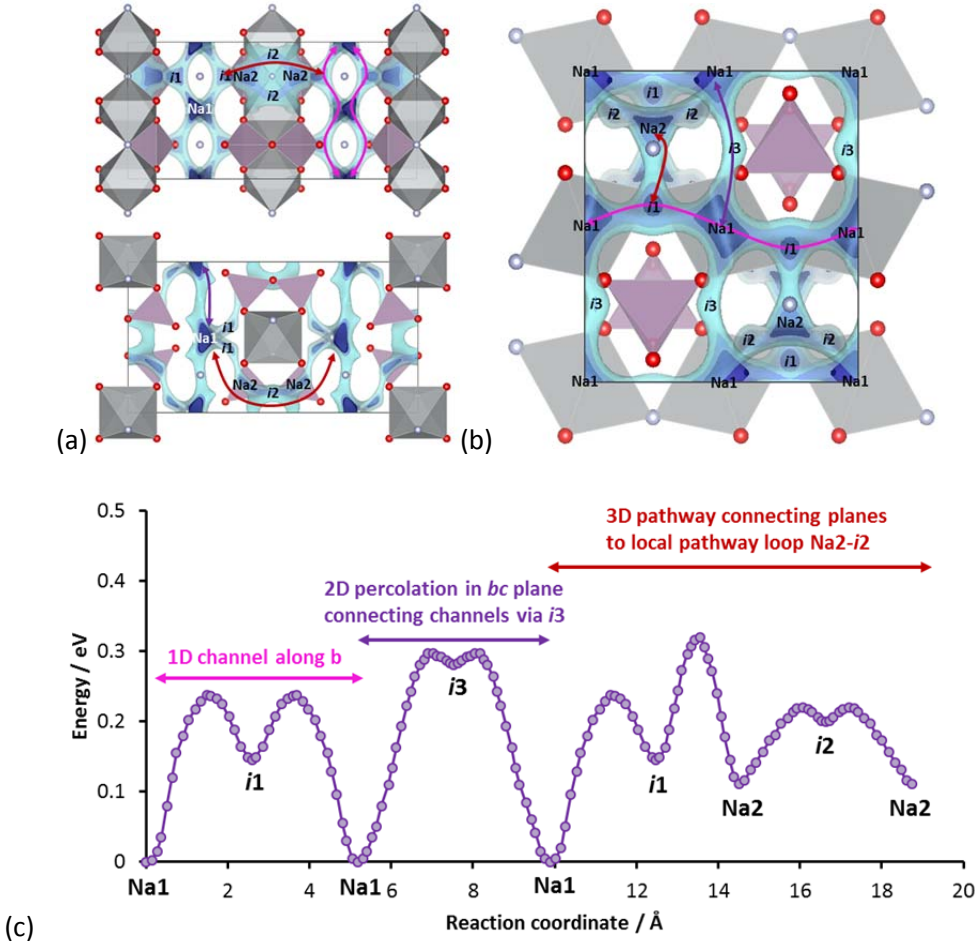

Fig. S8: Projection along (a) *c*- and *b*- (top and bottom respectively) and (b) along *a*-axis showing Na^+ migration pathways (represented by blue energy isosurfaces) in **$Na_4NiP_2O_7F_2$** (PO_4: purple tetrahedra, NiO_4F_2: grey octahedra, F: white spheres, O: red spheres. Coloured arrows indicate the lowest energy 1D (magenta), 2D (violet) and 3D (red) pathways for Na^+ ions in this compound). (c) Variation of the site energy along the relevant migration pathways involving two types of sodium sites as well as three types of low-energy interstitial sites. The displayed values refer (from left to right) to 1D migrations along the *b*-axis for the Na1 sites via interstitial site *i*1, the extension of the 1D path to a 2D pathway in the *bc* plane involving Na1 as well as interstitial sites *i*1 and *i*3 and finally the path connecting these planes to a 3D percolating network involving both Na1 and Na2 as well as *i*1, *i*2 and *i*3.

Besides the two fully occupied equilibrium sites we observe for $Na_4NiP_2O_7F_2$, three relevant (i.e. low energy) vacant interstitial sites *i*1 (at 0.353,0.250,0.429), *i*2 (at 0.500,0.611,0.857) and *i*3 (at 0.25,0.041,0.75). In accordance with the literature experimental data our bond valence site energy model of ion transport pathways (see Fig. S8) finds that the lowest energy pathway for Na^+ in $Na_4NiP_2O_7F_2$ is a 1D pathway along the *b*-direction connecting Na1 equilibrium sites via *i*1 and requires an activation energy of 0.24 eV, whereas with an activation energy of 0.30 eV the Na1-*i*1-Na1 are interconnected via *i*3 sites to form a two-dimensional pathway in the *bc* plane. Pairs of Na2 sites form a low energy local $(Na2\text{-}i2)_2$ pathway loop with a low barrier energy of *ca*. 0.1 eV and the connection of such loops to the *i*1 sites finally yields a 3D percolating Na^+ migration pathway network with an activation energy of 0.32 eV. Altogether the low activation energy for long-range transport along the *b* direction, the only slightly higher activation energies for migration in the other

directions as well as the availability of low energy interstitial sites within the migration pathways should qualify this material as a reasonably good Na ionic conductor fully in line with experimental findings. Following the same argument in the discussion of previous compounds, we thus expect this compound to exhibit significant capacity retention up to 10C cycling rate.